Journal of Colloid and Interface Science 657 (2024) 178–192

Contents lists available at ScienceDirect

Journal of Colloid And Interface Science

journal homepage: www.elsevier.com/locate/jcis

Tailoring the properties of poly(vinyl alcohol) "twin-chain" gels via sebacic acid decoration

Damiano Bandelli [a], Andrea Casini [b], Teresa Guaragnone [b], Michele Baglioni [b,c], Rosangela Mastrangelo [a], Luciano Pensabene Buemi [d], David Chelazzi [b], Piero Baglioni [b,*]

[a] Department of Chemistry, University of Florence, Via della Lastruccia 3, Sesto Fiorentino, FI 50019, Italy
[b] Department of Chemistry and CSGI, University of Florence, Via della Lastruccia 3, Sesto Fiorentino, FI 50019, Italy
[c] Department of Biotechnology, Chemistry and Pharmacy, University of Siena, Via Aldo Moro 2, Siena 53100, Italy
[d] Conservation Department, Peggy Guggenheim Collection, Dorsoduro 701, Venice 30123, Italy

GRAPHICAL ABSTRACT

Twin-chain (TC) PVA cryogels represent ideal candidate for applications in cultural heritage preservation but only moderately reported for such goals. In this contribution we introduce a simple, but robust design for the modification of PVA cryogels based on the reaction of functionalization of porogenic species with sebacic acid. The method proposed strongly affects the final gel's properties resulting in the preparation of materials with enhanced solvent compatibility, adaptability, and unprecedented cleaning efficacy also on modern/contemporary masterpiece from the Peggy Guggenheim collection, Venice.

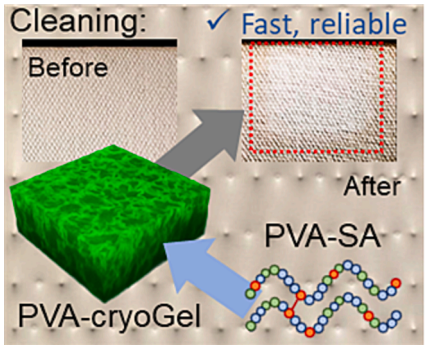

Abbreviations: PVA, Poly(vinyl alcohol); FT, freeze–thawing; TC-PNs, "twin–chain" polymer networks; SA, sebacic acid; *SEC*, size-exclusion chromatography; MALS, multi angle light scattering; RI, refractive index; M_w, weight-average molar mass; $Đ$, dispersity values; *CS*, conformational slope; α, α parameter of Mark–Houwink–Sakurada; ^{1}H NMR, proton nuclear magnetic resonance; *b*, blockiness; L_{OH}, average chain length of the vinyl alcohol fraction; R_g, radius of gyration; R_h, hydrodynamic radius; *U*, number of crosslinking per chain; [η], intrinsic viscosity; CLSM, confocal light scanning microscope; SAXS, Small Angle X-ray Scattering; USAXS, Ultra Small Angle X-ray Scattering; USANS, Ultra Small Angle Neutron Scattering; G', storage modulus; G'', loss modulus; EWC, equilibrium water content; FWI, free water index; MEK, 2-butanone; DEC, diethyl carbonate; pHEMA, poly(hydroxyethyl methacrylate); PVP, polyvinylpyrrolidone; TAC, triethyl-ammonium citrate; FTIR 2D, Two-dimensional Fourier-transform infrared spectroscopy; FPA, focal-plane array.

* Corresponding author.
E-mail addresses: damiano.bandelli@unifi.it (D. Bandelli), andrea.casini@unifi.it (A. Casini), teresa.guaragnone@unifi.it (T. Guaragnone), baglioni_michele@csgi.unifi.it (M. Baglioni), rosangela.mastrangelo@unifi.it (R. Mastrangelo), lpensabene@guggenheim-venice.it (L. Pensabene Buemi), david.chelazzi@unifi.it (D. Chelazzi), baglioni@csgi.unifi.it (P. Baglioni).

https://doi.org/10.1016/j.jcis.2023.11.093
Received 9 August 2023; Received in revised form 10 November 2023; Accepted 15 November 2023
Available online 21 November 2023

ARTICLE INFO

Keywords:
PVA
Polyvinyl alcohol
"twin-chain" gels
Sebacic acid
Crosslinking
Porogen
Hydrogels
Cultural heritage preservation

ABSTRACT

Hypothesis: The development of gels capable to adapt and act at the interface of rough surfaces is a central topic in modern science for Cultural Heritage preservation. To overcome the limitations of solvents or polymer solutions, commonly used in the restoration practice, poly(vinyl alcohol) (PVA) "twin–chain" polymer networks (TC-PNs) have been recently proposed. The properties of this new class of gels, that are the most performing gels available for Cultural Heritage preservation, are mostly unexplored. This paper investigates how chemical modifications affect gels' structure and their rheological behavior, producing new gelled systems with enhanced and tunable properties for challenging applications, not restricted to Cultural Heritage preservation.
Experiments: In this study, the PVA-TC-PNs structural and functional properties were changed by functionalization with sebacic acid into a new class of TC-PNs. Functionalization affects the porosity and nanostructure of the network, changing its uptake/release of fluids and favoring the uptake of organic solvents with various polarity, a crucial feature to boost the versatility of TC-PNs in practical applications.
Findings: The functionalized gels exhibited unprecedented performances during the cleaning of contemporary paintings from the Peggy Gugghenheim collection (Venice), whose restoration with traditional solvents and swabs would be difficult to avoid possible disfigurements to the painted layers. These results candidate the functionalized TC-PNs as a new, highly promising class of gels in art preservation.

1. Introduction

Nowadays, the development of materials capable of adapting to rough surfaces finds a vast landscape of applications from biomedical science to Cultural Heritage preservation.[1–4] The formulation of optimal systems depends on the type of application and on the characteristics of the target surface.[5,6] For instance, canvas and easel paintings, which are among the most iconic objects in Cultural Heritage, often exhibit a complex, rough surface resulting from the artist's painting technique, the degradation/alteration of binders and paint layers, and the uptake of dust and humidity, overall making the restoration of these artifacts a complex and delicate procedure. The restoration practice still partially relies on classic solvent and polymer chemistry, where solvent blends are selected based on their solubility parameters, and then applied either as non-confined or poorly confined in polymer thickeners.[7] This approach can pose the risk of swelling or leaching original components (binders, dyes) in the paintings, or leaving unwanted polymer residues on the treated surfaces, whose removal requires invasive rinsing steps.[7,8] In addition, some of the most widely employed solvents are petroleum-based, e.g. mineral spirits.[9].

Alternatively, effective and sustainable solutions have been proposed and assessed over the past decades in the framework of colloids and materials science.[9–11] Critical aspects of the cleaning systems, such as solvent entrapment and release behavior, adhesion, rheological properties, as well as macro– and microscopical features, should be specifically tailored for the preparation of materials with superior performances in the remedial conservation of artifacts.[12,13] In this context, hydrogels and organogels represent a turning point in conservation science, since they possess properties as cleaning capacities, [11,14–16] absorbers of volatile organic compounds (VOCs),[17,18] etc., protectives,[19] and sensing substrates,[20] making them a reference class of materials in the field of Cultural Heritage conservation. In particular, gels used to remove soil from painted surfaces must show high cleaning efficiency and allow for time–effective and non–invasive applications.[21] In addition to the final performances, a careful aspect to be considered is the nature of the components involved in the materials design.[22] In view of the growing socio–political interests on the development of green materials, features such as renewability, biocompatibility and biodegradability are more relevant than ever. [1,23].

Chemical hydrogels, i.e., able to upload aqueous solutions, tailored for art cleaning have firstly included crosslinked polyacrylamide and networks of poly(2-hydroxyethyl methacrylate) semi-interpenetrated with polyvinylpyrrolidone or polyacrylic acid (pHEMA/PVP, pHEMA/PAA semi-IPNs), which improved on traditional polymeric solvent thickeners in terms of enhanced mechanical properties and retentiveness.[9] However, while these gels perform well in the cleaning of flat surfaces, they are too rigid to homogeneously adhere to the rough surface of modern/contemporary paintings, a limitation also exhibited by gellan gels.[22] This issue was recently solved by developing a new class of hydrogels, the "twin-chain" poly(vinyl alcohol) (PVA) polymer networks (TC-PNs),[22] which have some key advantages over previous hydrogels. PVA is widely employed for the design of consumable goods thanks to its biocompatibility and moderate biodegradability,[24–26] and despite being usually considered petroleum–based, it can nowadays be produced from biobased ethyl acetate, resulting in a variety of eco–friendly polymers that are already commercialized (e.g. *Wacker*). In addition, PVA can be employed for the preparation of polymer networks with excellent resistance to mechanical stress, with or without the addition of molecules of interest for the target application.[6,27,28] The PVA TC-PNs, obtained by freeze–thawing (FT), were formulated using two types of PVA with different molecular weight and hydrolysis degree. [22] The presence of the two different PVA polymers induces phase separation and demixing in the pre–gel solution, which upon FT leads to a disordered, sponge–like interconnected porosity in the gel network as opposed to the hexagonally stacked channel–like pores of the single–component PVA gel.[22] In addition, the partially hydrolyzed PVA (hereafter referred as "additive") remains partially entrapped in the pore walls acting as a colloidal additive in the three-dimensional gelled system and increasing the mechanical compliance of the TC-PNs gel. These features are likely keys for the remarkable effectiveness that the TC-PNs gels demonstrated in the removal of soil or aged varnishes from Pablo Picasso's or Jackson Pollock's paintings, where the gel could adhere homogeneously to rough painted surfaces, granting homogeneous cleaning. Notably, the mechanical properties, the adaptability to rough painted surfaces, and the cleaning capability of the TC-PNs are critical factors that yield efficient and safe cleaning. Besides, these are physical gel networks prepared without solvents or crosslinkers but exhibit optimal mechanical and rheological behaviors typical of chemically crosslinked gels. Indeed, these systems allowed the safe and highly time-effective restoration of artifacts, which would have been highly risky or time-consuming using the traditional approach with non-confined solvents, polymeric dispersions in solvents, and cotton swabs.[21,22].

However, one important limitation of the TC-PNs is that, being hydrogels, their network has only moderate compatibility with organic solvents without being substantially altered or deteriorated. This hinders the application of these tools to numerous works of art that, being highly water-sensitive, cannot tolerate even the minimal contact with water.[16] While chemical gel networks of more lipophilic polymers are being progressively proposed,[29] the main rationale proposed in this contribution is to formulate a new class of PVA TC-PNs tuning their chemical modification to yield gel networks that maintain the optimal mechanical and retentive properties of the original twin-chain gels, while allowing the upload of organic solvents with different polarity.

This feature would open a new family of gels that lie in between hydrogels and organogels, keeping the most functional aspects of both classes and progressing over state-of-the-art formulations. From an applicative standpoint, the new gels would allow addressing the vastly diverse types of soil, grimes, coatings and overpaints that need to be removed from works of art in recurrent and challenging restoration interventions.

To this purpose, new TC-PNs were here formulated by functionalizing the PVA additive used in the twin-chain pre-gel solutions, tuning its hydrophobicity to modulate the phase-separation and demixing processes that drive the network gelation, overall resulting in different interfacial properties of the gels. In addition to using eco-friendly PVA, the functionalization should be carried out with natural or bio-derived compounds in the TC-PNs, to explore new classes of "green" cleaning tools.[30] Namely, we selected two commercially–available poly(vinyl alcohol–co–vinyl acetate) with similar molar mass but different vinyl acetate fraction (0.12 and 0.20) to be used as additives in the gel synthesis. Both additives were employed for a mild decoration reaction with the ecofriendly sebacic acid (see Scheme 1) and used in the freeze–thawing synthesis along with the fully hydrolyzed PVA. Sebacic acid is a derivative of castor oil, a renewable source that does not impact the food chain, and thus an optimal candidate to design "green" and sustainable functionalized networks.

A literature protocol for the thermal crosslinking of PVA[31–33] was here updated and complemented with extensive characterization of the process enabling the tailor–making of the final additives. The functionalized PVA additives produced cryogels whose microstructural features, e.g. polymer molar masses, crosslinking and water content, were characterized and correlated to macroscopic properties and the rheological behavior.

In view of favoring future applications in the Cultural Heritage conservation field, the structure to properties relationship study on the TC-PNs was complemented with their application on soiled painting mockups mimicking the rough soiled surface of actual modern/contemporary paintings. The cleaning effectiveness of the novel gels was evaluated through advanced macro–photography image analysis[34] and 2D Fourier Transform Infrared Spectroscopy Imaging. Finally, the most effective systems were used to clean a selection of canvas paintings (Peggy Gugghenheim collection, Venice), whose restoration with traditional approaches would have involved difficult and time-consuming step-by-step soil removal, using swabs and solvents under the optical microscope to avoid swelling or leaching of the painted layers.

2. Materials and methods

Poly(vinyl alcohol) with high degree of hydrolysis (99%, **P99**) was purchased from Sigma Aldrich. Two poly(vinyl alcohol-*co*-vinyl acetate) with an hydrolysis degree of 88 and 80% (**P88** and **P80**, respectively) were kindly supplied by Kuraray (POVAL™, 32–80 and 32–88). Sebacic acid (98.0%) was purchased by TCI chemicals·THF (anhydrous, ≥99.9%, inhibitor–free) was purchased from Sigma Aldrich. Ultrapure water was obtained by a Millipore MilliRO-6 Milli-Q gradient system (resistivity > 18 MΩ cm). All the other chemicals were purchased from common vendors with HPLC–grade purity. All chemicals were used without any further purification.

2.1. Instruments

Proton Nuclear Magnetic Resonance (^{1}H NMR) spectra were measured in DMSO–*d6* at room temperature on a Bruker AVIII400 UltraShield Plus spectrometer. The residual ^{1}H peak of the deuterated solvent was used for chemical shift referencing. Reaction conversion was calculated considering the integrals of sebacic acid (2.18 ppm) and the methyl protons vicinal to the ester bond (1.88 to 2.00 ppm). The conversion values obtained were employed for the calculation of the functionalization percentage and of the functionalization per chain according to:

$$Funtionalization\ percentage = f[\%] = Conversion \times FeedSA[\%]/F_{OH}$$

Where F_{OH} is the vinyl alcohol fraction in the copolymer and the Feed SA [%] is the feed of sebacic acid expressed as percentage;

and:

$$Funtionalization\ per\ chain = f_{chain} = Conversion \times FeedSA \times DP_n$$

Where DP_n is the degree of polymerization obtained from the number-average molar mass of P88 ($F_{OH} = 0.88$). The calculation of blockiness was performed employing ^{1}H NMR data. Briefly, three signals were taken as reference: the acetate signals (1.90 to 2.10 ppm); the signals of CH_2 protons related to vinyl acetate-vinyl acetate diads (AA, 1.70 to 1.90 ppm) and the remaining CH_2 protons related to vinyl acetate-vinyl

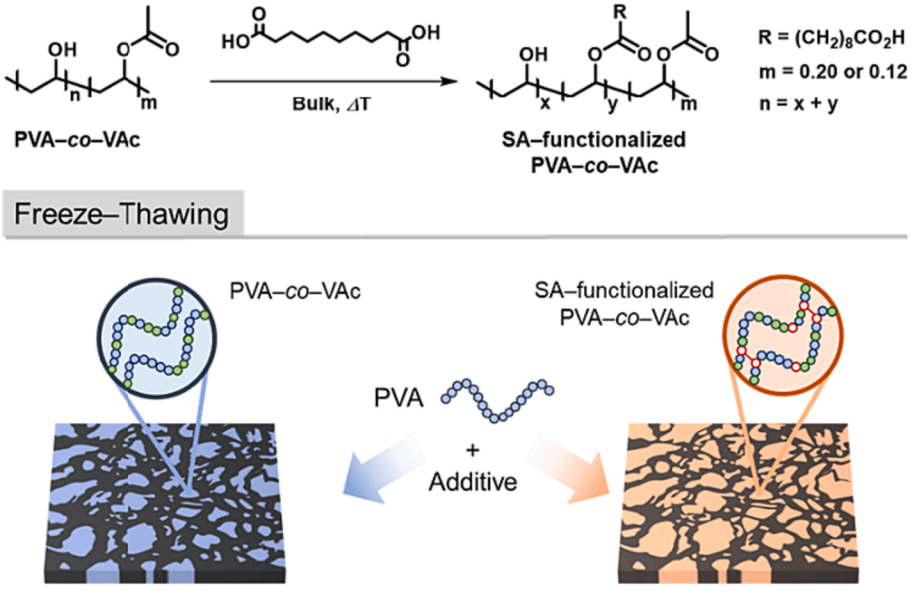

Scheme 1. Schematic representation of the crosslinking reaction of sebacic acid with two poly(vinyl alcohol–co–vinyl acetate)s and structural depiction of gel systems after Freeze–Thawing.

alcohol and vinyl alcohol- vinyl alcohol diads (AO and OO, respectively, from 1.11 to 1.70 ppm). Calculations were performed as reported in literature, integrating the areas of the signals, and normalizing them to calculate the blockiness and the average sequence lengths of vinyl alcohol and vinyl acetate blocks.[35–37]

Size Exclusion Chromatography (*SEC*) measurements were performed utilizing a system composed of a Shodex ERC–3215α degasser connected with a Waters 1525 binary HPLC pump, a Waters 1500 series heater set at 50 °C, a Wyatt miniDAWN TREOS detector, a Wyatt Viscostar–II detector and a Wyatt OPTILAB T–rEX detector, a Shodex pre–column GPC K_D–G 4A and a Shodex column GPC K_D–806 M employing a DMSO / DMF (70 / 30) mixture as eluent with a flow rate of 0.7 mL min^{-1}. A set of polyethylene oxide standards (PEO, 3 kg mol^{-1} < Mn < 969 kg mol^{-1}) samples were purchased from PSS (PEOkit) and used for calibration. All data evaluation was performed according to standard procedures employing ASTRA software.

Differential thermogravimetric (DTG) analysis was performed on a SDT650 Discovery (TA Instruments). Data were recorded from 30 to 230 °C at a heating rate of 10 °C min^{-1}.

Differential scanning calorimetry (DSC) measurements were performed with a DSC 2500 Discovery (TA Instruments) under a nitrogen atmosphere from −25 to 25 °C applying a heating rate of 0.5 °C min^{-1}.

Two-dimensional Fourier-Transform Infrared Spectroscopy (FTIR 2D) imaging was carried out using a Cary 620–670 FTIR microscope (Agilent Technologies), equipped with a focal plane array (FPA) 128 × 128 detector. The spectra were recorded directly on the surface of the samples in reflectance mode, with open aperture and a spectral resolution of 8 cm^{-1}, acquiring 128 scans for each spectrum. A "single tile" map has dimensions of 700 × 700 μm^2 (corresponding to 128 × 128 pixels) and a pixel size of 5.5 μm (i.e., each pixel has dimensions of 5.5 × 5.5 μm^2 and is related to an independent spectrum). In each 2D map, the intensity of characteristic bands of the samples was imaged. The chromatic scale of the maps shows increasing absorbance of the bands as follows: blue < green < yellow < orange < red.

Confocal laser scanning microscopy (CLSM) images were acquired using a Leica TCS SP8 confocal microscope (Leica Microsystems GmbH, Wetzlar, Germany). The chosen laser line was the Argon ion laser (488 nm laser line). Fluorescence was detected using photomultiplier tube (PMT) in the 498 to 540 nm range. The objective was a water immersion 63X/1.2 W (Zeiss). All samples were placed in the appropriate sample-holder (Lab-Tek® Chambered #1.0 Borosilicate Coverglass System, Nalge Nunc International, Rochester, NY, USA). For sample preparation, the target gel was immersed in a concentrated aqueous solution of Rhodamine 110 for 16 h.

Rheology measurements were performed on a Discovery HR-3 rheometer from TA Instruments (steel parallel plate geometry, diameter of 40 mm), equipped with a Peltier temperature control system. Prior to Frequency sweeps analysis, amplitude sweeps curves were collected in a range of oscillation strain between 0,01 and 50%, at a frequency of 1 Hz. Frequency sweeps analysis were set at a constant oscillation strain (1%) by increasing the oscillation frequency (0.01–100 Hz). The measurements were performed in triplicate at room temperature for each sample.

Small Angle X-Ray Scattering (SAXS) measurements were performed on the 10 m% solutions of P80, P88, P80SA, and P88SA, and on the four resulting gels G80, G88, G80SA, and G88SA. Scattering profiles were collected using a Xeuss 3.0 apparatus (Xenocs, Grenoble (France)), equipped with two position sensitive detectors (Q-Xoom) consisting of 1024 channels with a width of 54 μm, which are free to move on a rail in a chamber under high vacuum. The Kα radiation (λ = 1.542 Å) emitted by a Cu anode from the Genix 3D source was used. Calibration was performed concurrently with the analysis on the samples, using silver behenate (d = 58.38 Å). Scattering curves were obtained in the 0.004 and 0.5 $Å^{-1}$ q-range by merging the data collected with two different setups, using sample to detector distances of 0.3 m and 1.8 m. The temperature control was set to 25 °C and samples were measured in air. Polymer solutions were measured in 1 mm thick quartz capillary tubes sealed with hot-melting glue, while gels were analyzed in sealed cells with Kapton® windows (1 mm thick). Scattering curves were converted in absolute intensity (cm^{-1}), by measuring the scattering from a 1.6 mm thick glassy carbon reference specimen in the same experimental conditions. Finally, the experimental data were reduced by subtracting the scattering intensity from sample holder + water.

2.2. Initial reaction tests

Three 10 m/v% solution containing P88 (1.0 g each) was prepared in pure water and mixed with a 1 M solution of sebacic acid in THF to reach a sebacic acid to hydroxyl ratio of 0.5, 2.5 or 5.0 mol%. The obtained mixtures were dried in a oven set at 70 °C for 48 h. The obtained polymer films were heated from 70 to 120 °C in an oven with a heating rate of ~ 1.5 °C min^{-1}. The samples were removed from the oven after 1 h and analyzed by means of proton nuclear magnetic resonance, ^1H NMR, and size exclusion chromatography, *SEC*.

2.3. Reaction screenings

The same procedure described above was performed in order to prepare the sebacic acid-containing PVAs with both P80 and P88. The obtained polymer films were divided in pieces (around 250 mg each) and heated from 70 to 120 °C in an oven with a heating rate of 1.5 °C min^{-1}. The samples were removed from the oven when the temperature reached 120 °C (t = 0 h) and after 0.25, 0.5, 0.75, 1, 1.5, 2 and 4 h. Samples were analyzed by means of proton nuclear magnetic resonance, ^1H NMR, and size exclusion chromatography, *SEC*.

2.4. Upscale of the crosslinking reaction

The upscaled reaction of crosslinking was performed in a similar fashion as that described above for the reaction screenings. In a typical reaction route, 15.0 g of P88 were dissolved in 150 mL of pure water. The resulting solution was mixed with 7.14 mL (7.14 mmol) of a 1 M solution of sebacic acid in THF. The mixture was casted on petri dishes and the same thermal pretreatment previously described for the kinetic studies was applied. The polymeric films were heated to 120 °C for 1 h and let cooled down to room temperature. The upscale reaction resulted in two PVA decorated with sebacic acid P88SA and P80SA, respectively prepared from P88 and P80. The nomenclature "Px" is used to indicate all the additive serie.

2.5. Preparation of the PVA hydrogels

"Twin-chain" PVA/PVA gels were prepared following a procedure reported elsewhere, [22]where the PVA polymer with lower molecular weight (in our case P88 or P80, with or without decorations with SA) was originally used to induce the formation of a sponge-like disordered and interconnected porosity in the network of the PVA with similar molecular weight (P99). Thus, we will thereafter refer to P88 or P80 as the additive. A 10 m/v% solution of P99 in pure water was mixed with a 10 m/v% solution containing the selected poly(vinyl alcohol–co–vinyl acetate) (P88, P88SA, P80 or P80SA) in order to achieve a P99 to porogen ratio of 3 to 1. After 2 h of stirring at room temperature, the mixture was cast on plastic molds and transferred in a freezer set at –20.0 °C. After 16 h the resulting gels were defrosted at room temperature and were swollen in pure water for 1 week. The final materials are called G80, G80SA, G88, G88SA according to the nomenclature given to the additives Px. The nomenclature "Gx" is used to indicate all the gel series.

2.6. Swelling experiments

Swelling experiments of the samples obtained after freeze-thawing

(FT) were performed in order to assess both water entrapment and the release of the PVAs additives (P80, P80SA, P88 and P88SA) for a period of 1 week (168 h). The gravimetric determination of swelling capabilities was conducted to determine the evolution of weights of the cryogels over time. For this goal, square pieces of about 2 g (≈ 4 cm^2) were cut from each gel obtained from the FT of P99 with one of the porogens (P88, P88SA, P80 or P80SA). Each sample was immersed in 100 mL of pure water and was periodically weighted over 1 week (168 h). The swelling capability was obtained as follows:

$$\Delta m/m_0 = 100 \times (m_t - m_0)/m_0$$

where m_0 is the mass of the sample at time 0, m_t is the mass of the sample at time t.

The evaluation of porogen release was furthermore investigated via proton nuclear magnetic resonance (^{1}H NMR). Briefly, two solutions of 10 m/v% in D_2O containing P99 and the porogen were mixed to achieve a P99 to porogen ratio of 3 to 1. After 2 h of mixing, 1 mL of the resulting solution containing 150 mg of P99 and 50 mg of porogen, were cast in a 1.5 mL microcentrifuge tube (PP, Eppendorf) and transferred in a freezer set at –20.0 °C. After 16 h the resulting gels were defrosted at room temperature and were swollen in a 140 mM solution of acetone in 10 mL of D_2O for 1 week (168 h). During this time, samples were collected periodically and analyzed by means of ^{1}H NMR to obtain the porogen mass release and its conversion. The resulting values were employed for the calculation of the porogen release constant as well as for the determination of the process of transport of the additives in the gel matrix according to a first order kinetic model, the Peppas-Korshmeyer equation and the Weibull equation.

$$Release\,(m\%) = R_{max}\left(1 - e^{-kt}\right) \;\; \text{first order kinetic equation}$$

Where R_{max} is the maximum value for the release of the additives, k is the constant of release calculated and t the release time.

$$\frac{M_t}{M_\infty} = kt^n \;\; \text{Korsmeyer} - \text{Peppas approaches}$$

Where M_t is the mass released at time t, M∞ is the maximum mass released, k and n are factors related to the transportation process. In general, n values around 0.5 depict a Fickian transport, while $0.5 < n < 1.0$ is related to anomalous transport.

2.7. Water release experiments

Water release experiments were performed on the final Gx gels with surficial area of 2 × 2 cm^2. Briefly, the gels pieces were gently dried with towel paper (x2) and transferred on Whatman filter paper previously placed in a Petri dish. Subsequently, the Petri dish was covered with a lid to avoid evaporation. The amount of water released on the filter paper was recorded after the gel removal by weighing the Petri dish. Reported values are averages of 3 measurements.

2.8. Alkyd paint mock-ups preparation

Alkyd white pictorial mock-ups were prepared by spray painting panels of corrugated cardboard using an alkyd matte paint (Montana colors 94). The painted surfaces were let dry for 1 week, and then soiled by brushing with an artificial soil mixture reported in the literature, [30] comprising organic and inorganic particle dust suspended in nonane.

2.9. Cleaning tests

The PVA cryogels (G80, G88, G88SA, G80SA) were loaded with triammonium citrate (TAC 97%, Merck) water solution (5% wt.). Cleaning tests were performed by applying the gels directly onto the soiled painted surface. The gel sheets were divided into 3 × 2 cm^2 sheets and laid in contact with the soiled mock-up surfaces after being gently squeezed with blotting paper to remove the surficial water excess. The procedure was repeated up to three times on the same spot and took 2 min for each cleaning round (flipping the gel on the backside after 1 min), with no further mechanical action. The cleaning procedure was followed and validated by an in-house semi-quantitative assessment protocol previously developed by Casini et al.[34] and further optimized for this case study. For each gel application, a picture of the treated surface was acquired via Vis-light macro photography using a Canon EOS 5D Mark II Full Frame DSLR Camera and a Sigma 105 mm f/2.8 EX macro lens. The light configuration was 45° degrees along either side of the samples to minimize shadow casting on all analyzed substrates. Macro photos were analytically straightened with GIMP (GNU Image Manipulation Program) before ImageJ software processing,[34] allowing for the removal of the geometric distortions from the original picture and the retrieval of the correct dimensional information.

The original color channel photo-planes were then converted into grayscale images and binarized with the 17 threshold mathematical functions provided by ImageJ. The resulting images were thus subdivided into 64 × 64 pixel sub-areas, whose average grayscale values were thus correlated with the same portions of the original 8-bit images. As a result, from the cross-correlation analysis the threshold functions that yielded $R^2 > 0.95$ were kept, while the others were discarded. After measuring and averaging the percentage of black pixels across the chosen images, the results were normalized over the pristine soiled surface values and converted into a cleaning efficacy (%) simply by subtracting the normalized percentage of black pixels from 100.

Finally, the best performing gel formulation was assessed on an alkyd painted mockup mimicking modern/contemporary painting techniques, prepared using a commercial primed canvas, and oil (Windson&Newton) and alkyd colors (Ferrario). The mockup exhibits surface roughness in the order of 1–5 mm, similar to cavities and crests found in the paint layers of artists such as Jackson Pollock, Pablo Picasso, and others. The mockup was soiled with the same protocol as detailed before. Soil removal was carried out with the same procedure as for the white mockups, i.e. cleaning rounds of 2 min (1 min for each gel face) with no further mechanical action.

3. Results and discussion

3.1. Functionalization of PVAs with SA

The aim of the present work is to elucidate how selected polymeric additives can affect the morphology and the properties of TC-PNs PVA cryogels and their interactions with surfaces of interest in Cultural Heritage. To this purpose, two commercially available poly(vinyl alcohol–co–vinyl acetate)s (PVAs) with a vinyl alcohol fraction of 0.88 and 0.80 (P88 and P80, see Table 1), were reacted with sebacic acid (SA). Subsequently, either the commercially available P80/P88 or the SA-containing polymers were combined with P99 to produce different TC-PNs cryogels. In principle, the reaction of P80/88 with SA could produce the decoration of PVA chains, or even the formation of crosslinks where the SA function acts as a bridge between two hydroxyl groups of the polymer chains. Both these modifications are expected to affect the behavior of P80/88 during the preparation of the cryogels, in turn inducing effects on the final properties of the gels.

It is well known that even a low degree of post–synthetic crosslinking of polymers with relatively low initial molar masses can result in poor solubility, which in our case would impair or completely prevent the preparation of the pre–gel solution of P80/88 and P99, a fundamental step preliminary to the freeze–thaw (FT) gelation that yields the gels. Taking this issue into account, we employed a protocol of esterification developed for adipic acid and we updated it for sebacic acid.[31].

Essentially, preliminary reaction screenings were performed employing a 0.5, 2.5 and a 5.0 mol% feed of carboxylic acid moieties vs hydroxyl groups of P88, and monitoring the reaction conversion (%) as well as the water solubility and conformational parameters of the

Table 1
Selected structural characterization data of PVAs.

Code	Feed SA [mol %]	F_{OH}[a] [mol %]	M_w[b] [kg mol^{-1}]	$Đ$[b]	α[c]	CS[d]	b[e]	L_{OH}[e]
P88	0	88	217	1.57	0.65	0.57	0.49	17
P88SA	2.5	88	379	2.23	0.52	0.48	0.49	17
P80	0	80	240	1.48	0.69	0.54	0.43	12
P80SA	2.5	80	350	2.05	0.55	0.43	0.45	11
P99	0	≥ 99	220	1.26	0.72	0.57	–	–

[a] Fraction of vinyl alcohol in the (co)polymers (F_{OH}), estimated by ^{1}H NMR.
[b] *SEC*, eluent DMSO: DMF = 70: 30, absolute molar mass (M_w) via MALS detection, concentration from RI detection, and dispersity values ($Đ$).
[c] Parameter α of Mark–Howink–Sakurada, calculated as the slope of the log–log plot of the intrinsic viscosity [mL g^{-1}] vs absolute molar mass obtained *via SEC* analysis.
[d] Conformational slope (*CS*) calculated as the slope of the log–log plot of the radius of gyration vs absolute molar mass obtained via *SEC* analysis.
[e] b (blockiness) and L_{OH} (average chain length of vinyl alcohol units in the copolymer) calculated from ^{1}H NMR spectra according to literature procedures.

functionalized polymers after 1 h of reaction time (Figure S2). The conformation of the polymers was analyzed by means of size-exclusion chromatography (*SEC*) equipped with MALS–viscosimeter–RI detectors, extracting the polymers' α parameter in the Mark–Houwink–Sakurada equation, where $0.50 < \alpha < 0.78$ indicates a good solvent for the polymer.[38–40] Eventually, a 2.5 mol% feed was selected, which produced a decrease of α from 0.65 down to 0.52. Then, the duration of the functionalization reaction was optimized by checking over time the conversion extent of the reaction, the molar masses of the functionalized polymers, and their α parameter, for P88 and P80. The analysis of ^{1}H NMR data revealed for both polymers an initial slow conversion step within 0.5 h, while a steeper and linear increase of the conversions was detected up to 1.5 h (see Fig. 1). As expected, further increase of reaction time resulted in complete insolubility of the functionalized PVAs in water, making longer reaction times unsuitable for the scope of this work. The ^{1}H NMR analysis allowed extracting additional information according to procedures reported in the literature based on blockiness calculations.[35–37] Briefly, a blockiness value of 1 is related to random copolymers, while 0 indicates a perfect block copolymer. In our case, before functionalization, P80 and P88 featured similar blockiness values (0.43 vs. 0.49) but different average chain length of the vinyl alcohol fraction (L_{OH}, 12 vs. 17), suggesting that the two polymers have similar blocky structure but a varied composition. A constant copolymer composition and blockiness was maintained during the reaction with sebacic acid (Figure S5-S7). In principle, variation of blockiness could be ascribed to the increase or decrease of average chain lengths or to the degradation of the polymers via elimination pathways. Given the low sebaceate formation (conversion below 10 %), the constant blockiness values proved the absence of degradative steps during reaction.

SEC analysis of absolute molar masses revealed a slight shift of the chromatogram mode to lower elution volumes and the appearance of a high molar mass shoulder during the reaction of both P88 and P80 (Figure S8-S9). This indicates a slight increase in the weight–average molar mass (M_w) and dispersity values ($Đ$) (Fig. 1). In addition, using three detectors (MALS, viscosimeter, and RID) directly provided information on the polymer conformation in solution, namely the gyration (R_g) and hydrodynamic radii (R_h).

Despite the moderate increase of molar masses, we observed a decrease, during the reaction, of the conformational slopes (*CS*, i.e. the slope of the log–log plot of R_g, vs. the molar mass, and of the α parameter (Fig. 1, Figure S10-S13). This trend suggested that changes had occurred in the morphology of P88 and P80 and, therefore, in their solubility in the *SEC* eluent. This was further confirmed by changes in

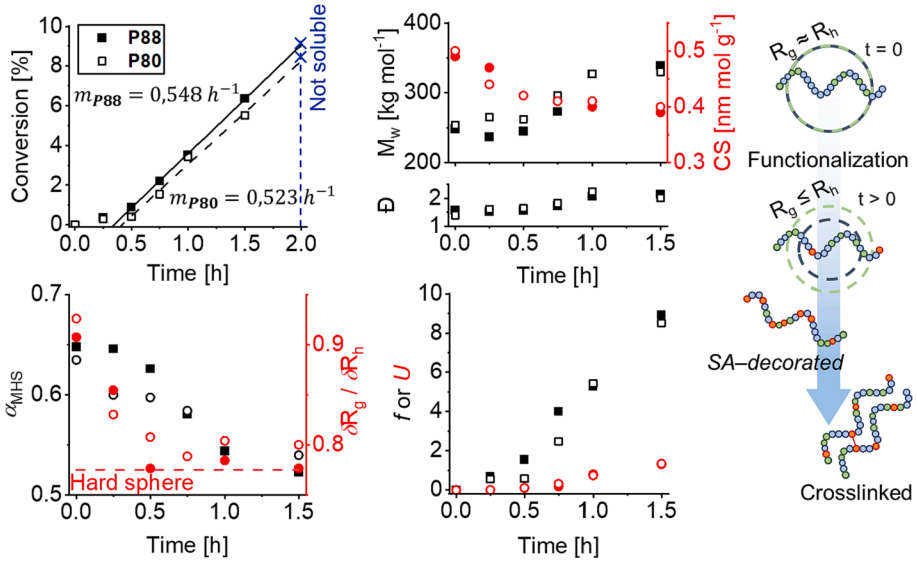

Fig. 1. Screening of the reaction of P88 and P80 with sebacic acid. **Top left:** Conversion over time, obtained via ^{1}H NMR analysis, of carboxylic acid groups into sebaceate, in P88 (solid symbol) and P80 (open symbol); the lines represent optical guidelines to help readibility. **Top middle:** Evolution of molar masses (M_w), of the conformational slope (*CS*) and of molar mass dispersity ($Đ$) over reaction time. **Bottom left:** Evolution of the parameter α of Mark–Houwink–Sakurada and of the slope of radius of gyration (R_g) vs. hydrodynamic radius (R_h) ($\delta R_g/\delta R_h$). **Bottom middle:** Evolution over reaction time of the functionalization number per chain [*f*] obtained from ^{1}H NMR analysis, and the number of crosslinking per chain (U) obtained from *SEC* analysis. **Right:** Schematic representation of the process of decoration and crosslinking of the PVAs P88 and P80 with sebacic acid.

the slope in R_g vs. R_h plots ($\delta R_g/\delta R_h$, see Fig. 1), which gives an estimation of how the polymer "softness" evolves by increasing the functionalization reaction time. Namely, $\delta R_g/\delta R_h$ decreased from values ~ 1 before functionalization (soft polymer particles) to values of 0.775 after 1 h, consistent with a hard sphere morphology.[41,42].

Overall, the observed variations of molar masses, solubility (α) and morphological parameters (slope of R_g vs. R_h), represent typical features of crosslinked systems in comparison with their linear counterparts. In addition, the extensive analytical setup showed that these features can be feasibly tuned simply by playing on the reaction time.

In principle, the observed variations of these parameters might also be due simply to the functionalization (decoration) of the PVAs with sebacic acid. To consider this possibility, we evaluated the number of crosslinking units per chain (U), described according to *SEC* procedures based on viscometry evaluation:

$$\left(\frac{[\eta]_{Crosslinked}}{[\eta]_{Linear}}\right)^{e} = \left[\left(1+\frac{U}{7}\right)^{1/2}+\frac{4U}{9\pi}\right]^{-1/2} \quad (1)$$

where $[\eta]_{Crosslinked}$ is the intrinsic viscosity of the crosslinked sample, $[\eta]_{Linear}$ is the intrinsic viscosity of the linear polymer, e is the draining parameter that was assumed equal to 0.75 for all the samples according to recent literature.[40] Usually, the U parameter is evaluated from the radius of gyration for both species; however, this method applies to samples with R_g higher than 10 nm that was not the case for the samples analyzed in this paper. Moreover, the use of this model requires that the molar mass of the two compared samples is the same. However, we verified that the Mark–Houwink–Sakurada parameters did not change significantly for P80 and P88 (before functionalization with SA) over a molar mass range between 90 and 270 kg mol^{-1}. Considering that the functionalization produces molar mass increases much lower that such range, the use of equation (1) is justified for the couples P80-P80SA and P88-P88SA. The value of U increased up to ~ 1.3 after 1.5 h of reaction, while the number of SA functions per polymer chain (f, obtained by ^{1}H NMR) is always 10 times larger than U for both P88 and P80 (Fig. 1). This suggests that most of the reacted sebacic acid is incorporated as a monoester, while only a small fraction can crosslink forming the diester species.

Having established an easily accessible and upscalable protocol for the decoration of P88 and P80, reaction upscales were performed at the same reaction conditions described above for 1 h. The final functionalized samples P80SA and P88SA featured overall similar composition (fraction of vinyl alcohol), blockiness and average chain length of vinyl alcohol units in the copolymer as their parent PVAs (see Table 1), while the α and the CS parameters decreased in a similar fashion as reported in the screening tests described above.

3.2. *PVAs gels formation*

Prior to gel formulation, semi-diluted solutions of the selected PVAs (10 m/v%) were analyzed by means of Small Angle X-ray Scattering (SAXS). Functionalization with SA did not produce dramatic changes for the dissolved PVAs, while some differences were ascribed to the different degree of acetylation (see SI). However, despite the similar behavior in solution, we hypothesized that the presence of sebacic ester moieties would impair the FT process when a PVA with high degree of hydrolysis was added to the polymers' solution due to the variation of interfacial properties between the polymeric components. To elucidate this aspect, the library of polymers P80, P80SA, P88, P88SA was employed as additive to highly hydrolyzed PVA (P99) for the preparation of "twin-chain" cryogels with a mass ratio of additive to P99 of 1 to 3 after freeze-thawing (FT), resulting in the gel series G80, G80SA, G88 and G88SA. The obtained hydrogels were swollen in water for one week to bring in solution all the fractions of PVA not included in the gel network.[22] The analysis of the swelling behavior and porogen release showed an increased swelling capability of the SA-containing gels (see SI). Moreover, G80SA and G88SA featured the highest rate of porogen release, suggesting that functionalization of the additive can hinder its inclusion in the P99 gel network, possibly owing to a more marked phase separation between the polymers in the pre–gel solution. In all cases, modeling the release over time with the Weibull equation provided better fittings than the first order and Korsmeyer–Peppas functions (see SI). The fitting results suggest that the transport mechanism of the additive in the P99 matrix is mainly Fickian diffusion, with slight contributions of case-II transport (polymer chain swelling in the matrix) for G88SA and G80.

Further information on the structural changes induced by the porogenic materials were obtained analyzing the cryogels via confocal microscopy after 1 week of swelling, employing Rhodamine 110 as fluorophore (see Fig. 2). The analysis revealed the presence of a disordered sponge–like interconnected porosity for all the samples investigated, in agreement with previously reported data on similar twin–chain PVA gels.[22] Patterns of dense regions alternated with interconnected porosity are observed in the non-functionalized networks.

A quantitative analysis of the pore and gel phase was performed via chord analysis. Briefly, 80 planes of each 3D image from confocal microscopy were binarized, and chords were extracted as randomly oriented segments connecting phase boundaries for the continuous gel phase and the pore phase. The frequency of chords vs their size (R) was plotted for pores (Fig. 2) and walls (**Figure S17**). The slope of the so-obtained curves allows calculation of a characteristic dimension, λ, for pores and walls in each system (Table 2).[43,44] λ can be described as the chord dimension most likely occurring in the pores or chord phases. Due to image resolution, the minimum chord length was set to 2 μm.

The pores chord distribution shows a slight bump for 6.5 μm < R < 9.5 μm, suggesting a certain abundance of pores sizes in this range in all the investigated systems. On the other hand, the intercept of experimental data with the X-axis and the area under each curve at lower frequencies indicate the presence of larger pores with sizes differing among the systems. More specifically, the highest limit of pores sizes varies according to the following trend: G88 > G80 > G80SA > G88SA. The half cumulative relative abundance of pore size (P50, see Fig. 2) follows the same trend, indicating that functionalization of PVA with SA causes a reduction of the average pores size. This could be the effect of different P80/88 chains self-interaction after decoration and, thus, different domains produced by the polymer–polymer phase separation in the pre-gel solution. Therefore, despite the similar packing of PVA chains in semi-diluted solution observed through SAXS, changes in the polymer architecture modified the final gels' morphologies and pores' size. The average walls size is very similar for the four systems, therefore we excluded that this parameter could explain differences in the transport properties among the gels; however, being λ_{Walls} very low, its accurate estimation is limited by the resolution of the confocal images.

The nanostructure of the four gels was then characterized by means of SAXS analysis. Fig. 3 shows the scattering profiles of the samples, together with their best fitting curves.

Small Angle X-ray Scattering (SAXS) data collected on the TC-PNs were fitted using a modified version of the approach originally proposed by Hudson et al.[45] to fit Ultra Small Angle Neutron Scattering (USANS) curves of PVA gels. However, since USANS covers a q range that allows access to characteristic lengths of 10 μm in the gels, Hudson et al. used a model to account for such long–distance interactions, which included a mass fractal structure factor. In the present work, in order to fit the scattering intensity in the low–q region there was no need for a structure factor, thus the fitting function was modified as follows:

$$I(q) = \frac{A}{\left[1+\frac{D+1}{3}\left(q^2\xi^2\right)\right]^{D/2}} + Be^{\frac{-q^2R^2}{3}} + \frac{C}{\left(1+q^2\chi^2\right)^n} + bkg \quad (2)$$

where A, B, and C are scaling parameters, and, according to Hudson et al.[45] on similar systems, the three terms account for different

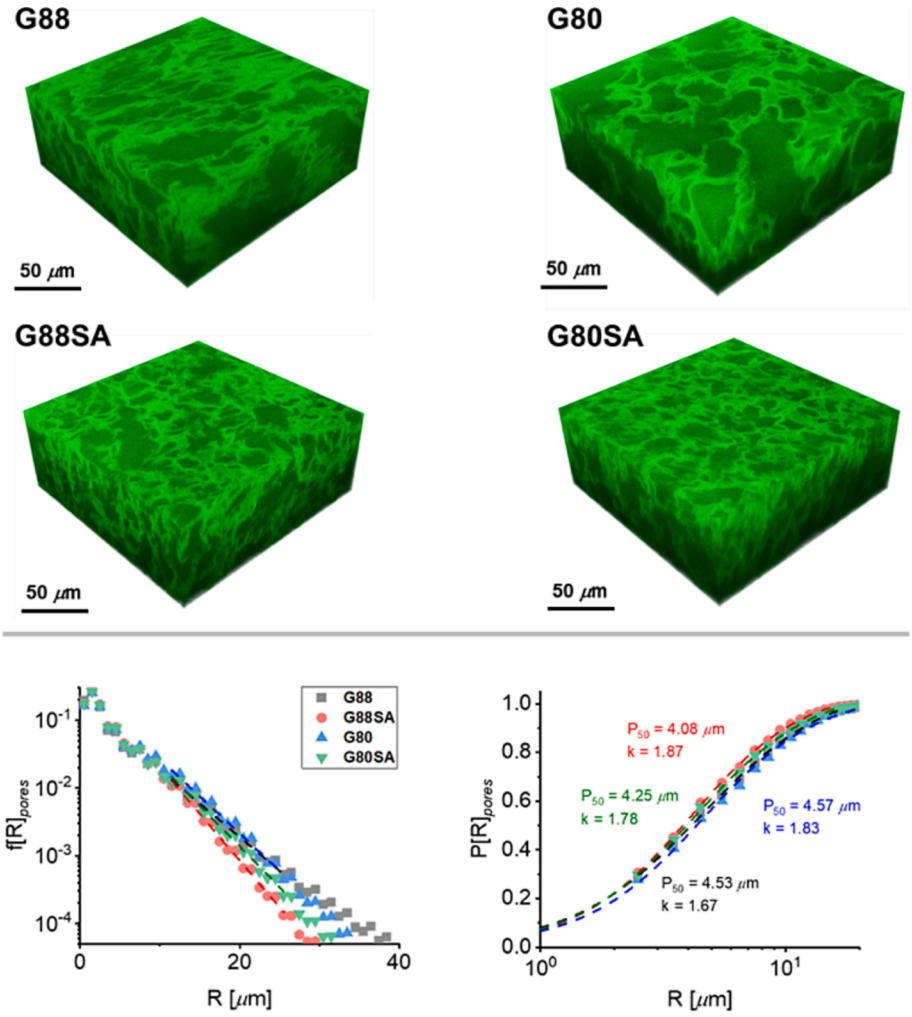

Fig. 2. Confocal microscopy images of PVA–based hydrogels swollen for 1 week in pure water, loaded with an aqueous solution of rhodamine 110 and obtained employing a Px to PVA (P99) mass ratio of 1 to 3. **Top:** Raw images. **Bottom Left:** Plots of relative abundance *f[R]* vs. size (*R*) of the pores, obtained via chord analysis and fitting according to $f[R] \propto e^{-R/\lambda}$. **Bottom Right:** Cumulative abundance *P[R]* vs. length (*R*) of the pores, obtained via chord analysis and fitting to $P[R] = R^k/(R^k + (P_{50})^k)$, where P_{50} represents the half cumulative relative abundance.

Table 2
Main fitting parameters obtained from the chord analysis of CLSM images and from SAXS patterns of the PVA gels.

Code	Confocal microscopy [a]		SAXS [b]		
	λ_{Pores} [μm]	λ_{Walls} [μm]	ξ [nm]	R [nm]	χ [nm]
G80	4.1 ± 0.1	1.4 ± 0.1	38.4 ± 0.9	5.6 ± 0.6	8.1 ± 0.7
G80SA	3.7 ± 0.1	1.3 ± 0.1	24.1 ± 0.5	7.9 ± 3.4	6.1 ± 0.5
G88	4.1 ± 0.1	1.4 ± 0.1	78.2 ± 0.5	6.2 ± 0.2	7.5 ± 0.1
G88SA	3.2 ± 0.1	1.3 ± 0.1	31.8 ± 0.4	6.0 ± 0.2	7.1 ± 0.2

[a] The parameter was extracted as the slope of the fitting of the frequency of chords vs their size according to $f[R] \propto e^{-R/l}$ depicted in Fig. 2 for pores.
[b] Parameters calculated from SAXS patterns according to **equation (2)**. For all the gels $D = 4.0 \pm 0.1$ and $n = 1.5 \pm 0.1$. Where ξ is the size of large polymer blobs structures, *R* is the size of crystallites in the polymer network and χ is the size of non-gelled regions.

characteristic lengths and physical structures in the gel network. χ can be described as the size of non-gelled regions where PVA chains are less constrained in a liquid-like environment; R represents the size of crystallites in the polymer network; ξ is a measure of the size of larger structures, possibly polymer clusters or even pores. D is related to the surface fractal dimension ds by the relation ds = 4 - D/2, while 2n is a surface fractal Porod exponent at high q.

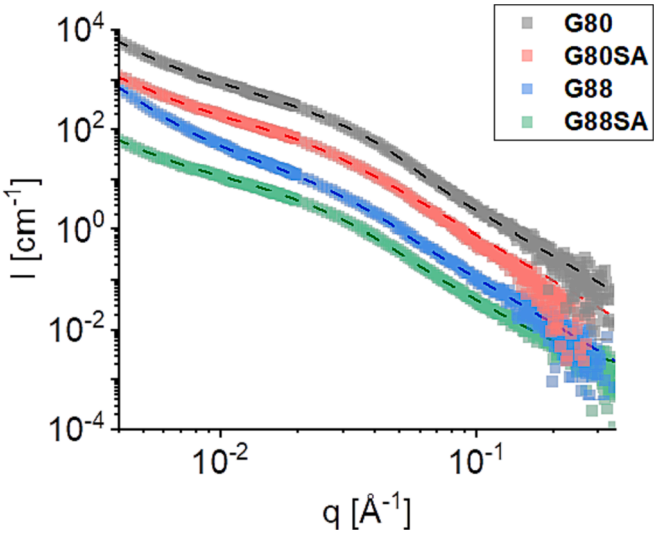

Fig. 3. Scattering profiles of G80, G80SA, G88, G88SA gels. Fitting curves are represented as dashed lines and were obtained according to equation (2). The experimental curves have been arbitrarily offset for sake of clarity.

The fitting parameters reported in Table 2 show that D = 4 (and thus ds = 2) for all the gels, which is an indication of flat surface structures in the medium–low-q range. On the other hand, at higher q the slope of the scattering curves slightly changes (see Fig. 3) and a Porod exponent of 2n = 3 was found for all the gels, which accounts for a rough surface, most likely due to the presence of the swollen PVA network in the liquid-like disordered regions of gels' walls. G80 and G88 present similar structures at the nanoscale, with PVA crystallites and PVA domains in the liquid-like regions having almost the same size (R ≈ 5–6 nm, and χ ≈ 7–8 nm, see Table 2). However, G88 has significantly larger (almost twofold) PVA structures at a larger scale. This might be attributed to the presence of the more hydrophilic P88, which gives lesser perturbation of the gel formation process (P80 phase separates more easily during the gelling at low temperature), resulting in longer-range order of larger PVA structures. This effect is also present when the SA-modified PVAs are used as porogens. In particular, the presence of P80SA in G80SA further decreases the size of large PVA characteristic lengths, while P88SA lowers ξ to almost the initial value of G80. This is a clear indication of how the modification of the intercalating polymers can be used to tune the gel nano- and, subsequently, micro-structure and porosity. At a finer scale, G80SA and G88SA are not much different from G80 and G88, meaning that the presence of crosslinks and sebacic acid residues on P80SA and P88SA only slightly affects the size of P99 crystallites and the structure of the liquid-like non-gelled regions within gels' walls. More in detail, G80 is the polymer gel network where the effect of the SA modification on the gelling process is more evident (i.e., R increases from 5.6 to 7.9 nm, and χ decreases from 8.1 to 6.1 nm), as a result of the addition of P80SA (i.e., the most hydrophobic of the PVA additives).

The effects of these structural features on the mechanical properties of the gels were analyzed by means of rheology. Preliminary amplitude sweep analysis revealed that, regardless the cryogel, the storage modulus (G') and the loss modulus (G'') featured a linear behaviour in the investigated range of oscillation strain. For this reason, an oscillation strain of 1% was chosen to perform frequency sweep experiments (Fig. 4). Similar values of both G' and G'' were obtained for the P80-based systems, while a significative variation was obtained for G88SA, which shows higher G' and G'', and G88 that featured the lowest values (see Table 3).

A comparison with the micro and nano-structural data obtained from both CLSM and SAXS analysis suggested that, for G80, functionalization and changes in structural features result in reduced stiffness. This likely enhances the material adaptivity to surfaces, since lower G' and G'' values favour the adhesion of the gels to rough surfaces. Along with the presence of large, interconnected pores in the gel network, these features were expected to promote the removal of dirt. In all cases, the gels have lower storage and loss moduli than twin–chain PVA gels previously reported (which used PVA additives with lower molar mass) and of other gelled networks proposed in art conservation,[15,46–49] but maintain good resistance to traction and handling as showed by previous PVA gel networks.[22,30].

Table 3
Selected structural characterization data of PVA–based gels.

Gel code	Polymer code	**P99** to $\mathbf{P_x}$ mass ratio	*EWC*[c] [%]	*FWI*[d]	G'[e] [Pa]
G88	**P88**	3: 1	97	0.92	70.7
G88SA	**P88SA**	3: 1	97	0.92	372.6
G80	**P80**	3: 1	96	0.93	266.2
G80SA	**P80SA**	3: 1	97	0.92	202.4

[c] Equilibrium water content in the fully hydrated hydrogel estimated *via* DTG measurements.

[d] Free water content evaluated according to:(34)$FWC = \Delta H_{m,H2O}/EWC \times \Delta H^{*}_{m,H2O}$

[e] G', Storage modulus obtained from rheology measurements at 1 Hz.

Finally, a central requirement for gels employed in art cleaning is the capability of uploading large amounts of water and other solvents, which can then be released in a controlled fashion at the gel–artifact interface. All the gels synthesized in this study show optimal water uptake, with equilibrium water content (EWC) of ~ 97%, and free water index (FWI) of ~ 0.92 (see Table 3). Additionally, we let the water-swollen cryogels equilibrate in a series of organic solvents with different polarity, common in art cleaning interventions, i.e., acetone, diethyl carbonate, 2-butanone and 1-pentanol. Exposure to a 20 v% solution of acetone in water resulted in a weight plateau of 120 m% for G80 after 4 h of swelling (Fig. 5). Similarly, G80SA and G88SA reached a plateau of 110 m% in the same time span, while G88 did not vary its original weight upon solvent exchange. A similar behaviour was detected when gels were immersed in diethyl carbonate, with a plateau reached at 110 m% for G80 and no weight variations for the others. In contrast, exposure to 2–butanone and amyl alcohol resulted in a weight decrease (shrinkage) for all the investigated systems. G80SA featured the lowest mass decrease (loss of 25–30 m%) but maintained good mechanical properties. Overall, despite being hydrogel systems, G80,

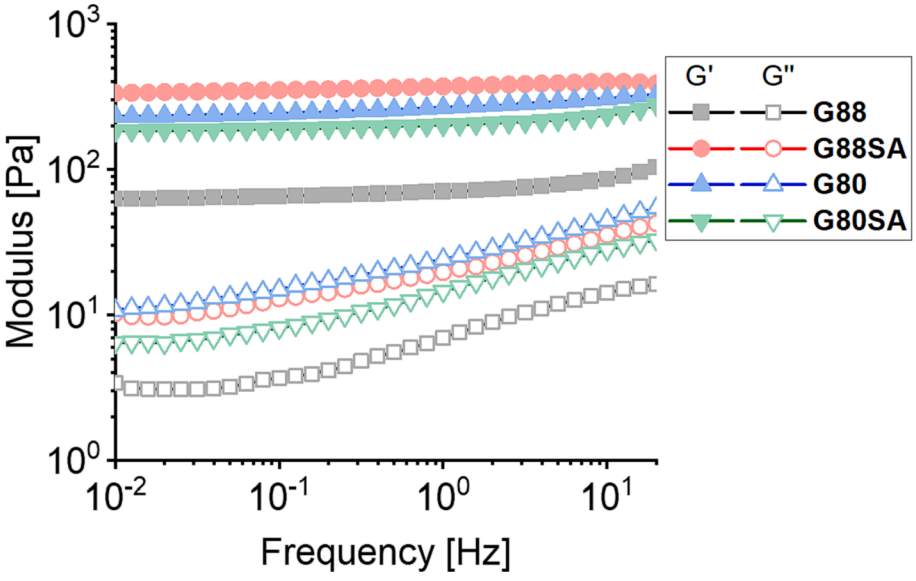

Fig. 4. Frequency sweep analysis of G80, G80SA, G88, G88SA gels.

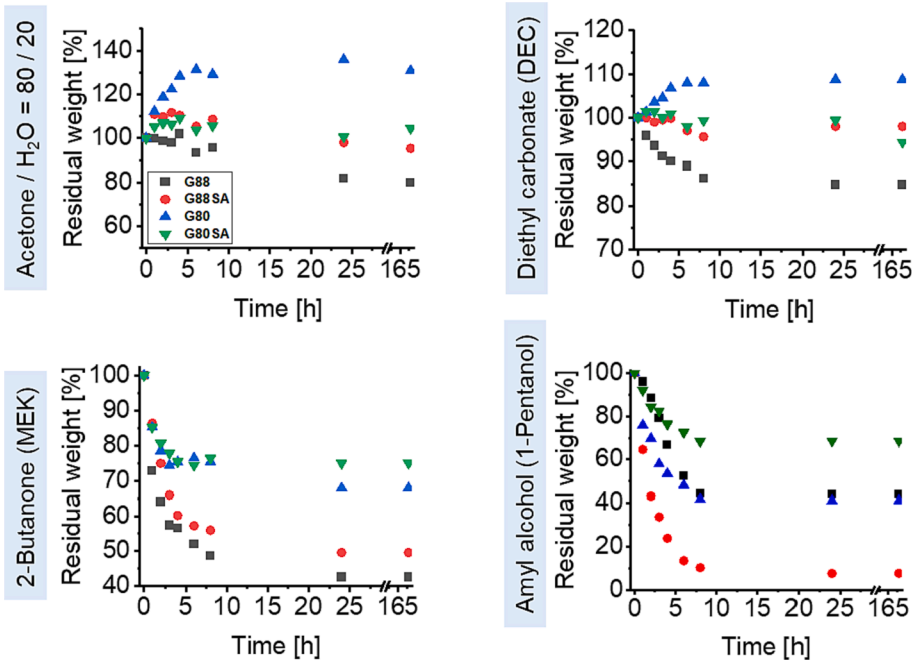

Fig. 5. Gravimetric solvent exchange of the cryogels G88 (Black), G88SA (Red), G80 (Blue) and G80SA (Green) performed at room temperature for 1 week (168 h) for different solvents. **Top left:** Swelling in a 20 v% solution of acetone in water. **Top right:** Swelling in diethyl carbonate. **Bottom left:** Swelling in 2-butanone. **Bottom right:** Swelling in amyl alcohol. (For interpretation of the references to color in this figure legend, the reader is referred to the web version of this article.)

G80SA and G88SA showed good solvent exchange capability, while G88 showed the poorest uptake of pure organic solvents. In particular, the functionalization with sebacic acid significantly improved the capability of the twin–chain gels to upload organic solvents with various polarity. *This is deemed as an advantageous feature, since it expands the range of cleaning applications in art conservation, where several artifacts are covered with unwanted layers of various hydrophilicity/hydrophobicity (aged varnishes, particulate or sebum soil, overpaint vandalism, etc.).*

Aiming to employ the **Gx** gel series for applications in Cultural Heritage, a central feature, beside solvent compatibility, is the controlled release of the target cleaning fluid at the gel's surface. In this regards, water-based fluids (e.g. aqueous solutions and suspensions) represent intriguing cleaning systems due to their safe handling and high versatility. For this reason, water release experiments were conducted on a model substrate (Whatman paper) put in contact with the gels until saturation, to access both the release behavior and the mechanism of transport of solvent in the gels (**Figure S18**). After 1 min application, all the Gx series featured a release of around 5 mg cm^{-2}. Increasing the application time up to 5 or 10 min, the release rate reaches 17–23 mg cm^{-2}, still a safe value to avoid excessive wetting of water-sensitive surfaces, and comparable with those of highly retentive pHEMA/PVP gels used for restoration.[50] These application times are representative of those actually used in cleaning operations on easel paintings.

Overall, the evolution of water release for the Gx series was fitted according to the model proposed by Korsmeyer–Peppas (see **equation S3**) to access the mechanism of solvent transport (**Figure S18**). For G80, G88 and G88SA, values of the n parameter equal or below 0.5 were obtained, suggesting Fickian diffusion. A slightly higher n value of 0.60 was obtained for G80SA hinting to anomalous transport. No satisfactory fitting could be obtained in this case using the Weibull equation.

After demonstrating the effect of functionalizing PVA with SA on the twin–chain gels' nano– and microstructural features, mechanical properties, and solvent compatibility, we tested the gels for the removal of dirt from mockups representative of modern/contemporary painted surfaces.

The pH values of water loaded in each Gx sample ranges from 6.62 to 6.80. Overall, pH values close to neutrality represent optimal conditions to avoid degradation of the treated surface.[51] Subsequently, the gelled systems were let equilibrate in a 5 wt% solution of triethyl-ammonium citrate (TAC) overnight prior to use. To achieve soil removal, the gels were simply put in contact with the soiled surface, and then removed, without any additional mechanical action.

The different Gx gel formulations were assessed on white alkyd paint mockups (see Matherials and Method section) to compare their cleaning efficacy on homogeneous white background surfaces with no pronounced roughness. Results (see Fig. 6) showed that G80SA exhibited the best cleaning performance right after the first application, with soil removal already close to 100%, marking a relevant improvement over the non-decorated benchmark. After there applications, also G80 and G88SA reach a comparably good soil removal, while G88 proved to be the less effective system (soil removal ca. 90% after three applications).

The cleaning effectiveness of twin-chain PVA cryogels was previously attributed to the presence of a sponge-like disordered and interconnected macroporosity, where large pores and microcavities enhance the capture of dirt at the gel–paint interface and its inclusion in the gels. The interconnected porosity might also favour the capture and retaining of soil by the gel network during the cleaning application, when evaporation at the gel upper surface is expected to recall water from the bulk through the interconnected pores, promoting dirt pick-up. The optimal performance of G80SA among the most effective Gx formulations, can be explained as a balance of different factors in addition to the sponge-like porosity. First, the slightly lower pore size could enhance capillarity suction in the gel network. Second, its lower elastic modulus makes it more compliant and likely favours adhesion to rough surfaces and, thus, homogeneous soil removal. Moreover, the slightly higher water release favours effective wetting of the gel-soiled paint interface. Finally, G80SA has the highest hydrophobicity (highest swelling capability in partially hydrophobic solvents), which along with the sponge-like pore network can boost the removal of the hybrid hydrophilic-hydrophobic soil. These results prove that small tweaks in the physico-chemical properties of the gels can deeply impact their cleaning effectiveness.

FTIR 2D Imaging confirmed complete soil removal at the micron scale, while no PVA residues (**Figures S19-S20**) were left onto the cleaned paint surfaces, down to a detection limit of the FPA detector, i.e.

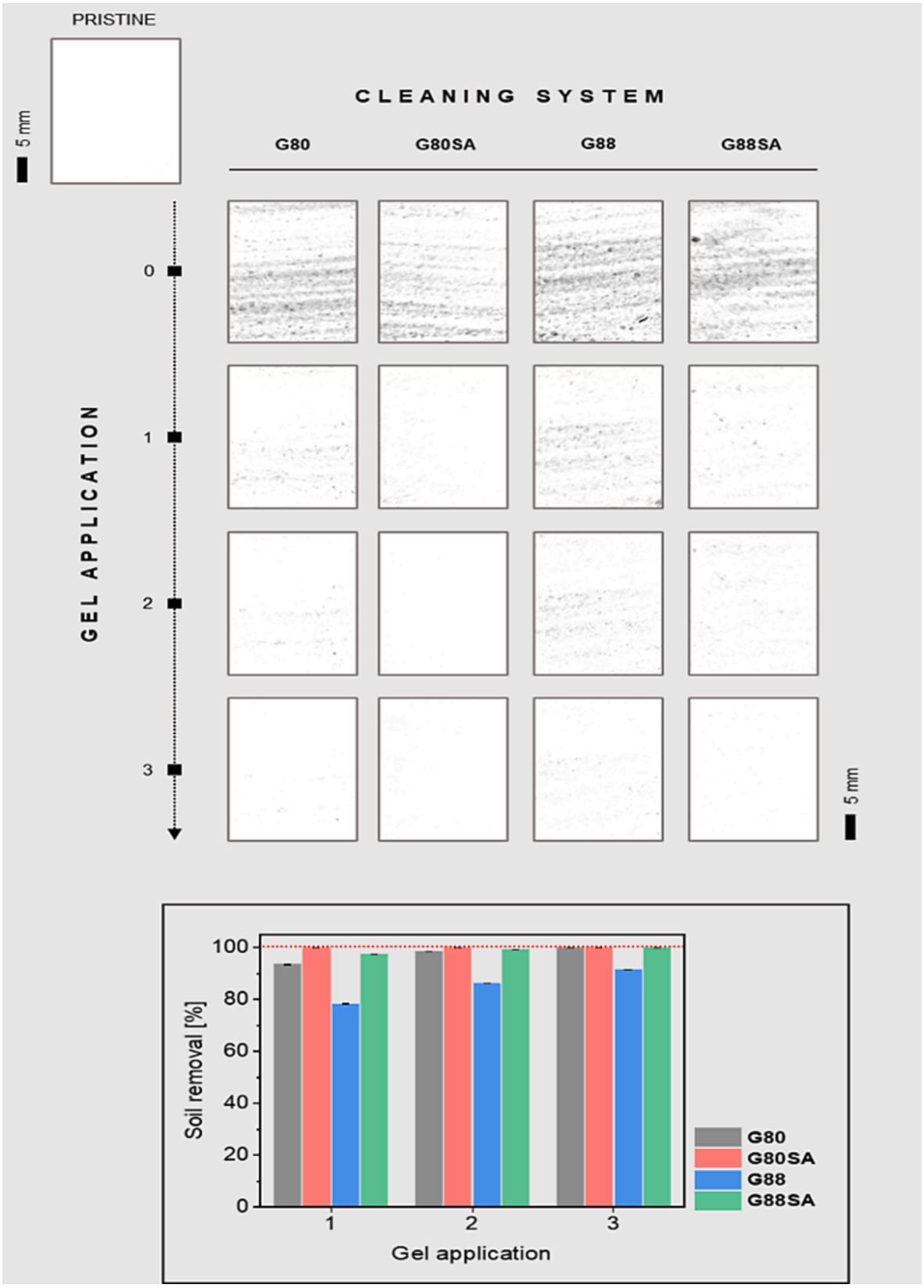

Fig. 6. Photographs of the area treated with the gels systems Gx loaded with a 5 wt% aqueous solution of TAC, and evaluation of soil removal from white alkyd paint mockups. **Top left:** Image of pristine alkyd-white painted surface. **Main top panel:** Assessment of the cleaning capability of, from right to the left, G80, G80SA, G88 and G88SA. From top to bottom, each row represents the non-treated soiled mockups (0 gel applications), and the surfaces after 1, 2, and 3 cleaning steps, respectively. **Bottom:** Soil removal percentage for each gelled system (Gx) after 1, 2, and 3 applications obtained via a semi-quantitative image analysis (see SI).

ca. 0.02 pg/μm^2.[22].

The G80SA cryogel provided optimal soil removal also on the cadmium red alkyd mockup representative of typical paint layers such as those found in modern/contemporary art (see Fig. 7), whose increased surface roughness with cavities and crests in the range of 1–5 mm typically hinders soil removal with traditional rigid gels such as gellan gum or agar.[22] Three cleaning applications of 2 min (1 min per side) were performed without any additional mechanical action, i.e. relying only on the action of the gel to remove the soil. The cleaning procedure allowed the recovering of the painting original texture, with homogeneous removal of the artificial soil, as highlighted by macrophotograpy (Fig. 7) and FTIR 2D imaging (**Figure S19-S20**). In the latter case, mapping the OH-stretching (νOH) bands of kaolin (artificial soil main component) in the 3725–3592 cm^{-1} region prior and after cleaning, demonstrated the quantitative removal of artificial soil down the micron scale.

Overall, G80SA proved to have optimum capability to treat flat as well as rough surfaces during cleaning interventions. Finally, the G80SA hydrogel was used to clean a series of paintings from Gastone Novelli ("Ha vinto il Bologna", 1964 – The Bologna Team Won the Match), Enrico Castellani ("Superficie Bianca", 1977 – White Surface) and Mario Sironi ("Il ciclista", 1916 – The Cyclist) belonging to the Peggy Guggenheim Collection (Venice) (Fig. 8). The three selected paintings were affected by soil (Novelli, Castellani) or aged varnish (Sironi), which had produced discoloration and paint degradation over the last decades. Importantly, the paintings' surface features and sensitiveness to solvents, made the removal of soil/varnish particularly challenging and risky with conventional cleaning tools such as poorly confined solvents and cotton swabs.

In other words, conventional cleaning would involve time-consuming cleaning steps working under the microscope to avoid, at each stage, the swelling or leaching of paint layers. Instead, the application of G80SA (with the same protocol as on the painting mockups,) resulted in the feasible and safe removal of dirt or aged varnish layers, recovering the original hue of the colors with no alteration of the paints. The gels were used loaded with TAC for the removal of surface soil, and with the solvents to remove aged varnish layers. Soil and solubilized varnish migrate inside the gels, as highlighted by their discoloration (see Fig. 8, panel Y1-2).

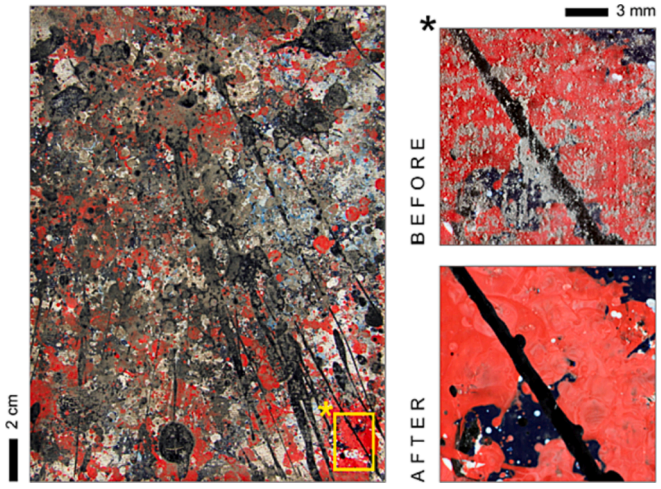

Fig. 7. Cleaning tests on an alkyd mockup with increased surface roughness, representative of typical paint layers found in modern/contemporary art. Soil removal was performed employing the G80SA gel loaded with a solution of TAC (5 wt%). **Left:** Image of the overall sample, the rectangular area boxed in yellow was treated with G80SA. **Top right:** Zoom-in in the region of gel's application prior to the cleaning procedure. **Bottom right:** Zoom-in in the region of gel's application after the cleaning procedure. (For interpretation of the references to color in this figure legend, the reader is referred to the web version of this article.)

Such safe and effective cleaning by the new gels allows carrying out highly time-effective interventions, without the need of time-consuming steps to check detrimental effects on the paints as would occur with the traditional methodologies based on classic solvents and polymer thickeners.

Overall, the new "twin-chain" PVA gels exhibit enhanced performances and versatility, owing to the functionalization with sebacic acid, and improved sustainability, thanks to the use of biobased PVA polymers and SA. These features candidate the SA-modified hydrogels as new promising tools in the palette of solutions available to art conservators, fostering the safe restoration of works of art and their transfer to future generations.

4. Conclusion

In a previous paper [15], for the first time, was reported on a new class of gels named "twin-chain hydrogels". These hydrogels have been demonstrated to be the most performing systems for the cleaning of modern and contemporary artifacts as paintings by Pablo Picasso and Jackson Pollock.[21,22] The twin-chain hydrogels are formed by PVA polymer chains with different molecular weight, taking advantage of a liquid–liquid phase separation during the gels cryo-formation. In the present paper we demonstrated for the first time the possibility of functionalizing chains of PVA with sebacic acid to tune changes in the micro–, nano-structure, and rheological properties, of "twin–chain" PVA/PVA gel networks. Our aim was to expand the possible applications of this class of hydrogels (which outperforms conventional cleaning tools),[22] tuning their mechanical properties and their capacity to upload solvents of interest in cleaning operations, as in the conservation of Cultural Heritage items. In particular, two commercially available PVAs with hydrolysis degree of 80 and 88%, either pure (P80, P88) or functionalized with sebacic acid (P80SA, P88SA), were used along with fully hydrolyzed PVA in freeze–thaw synthetic processes to form the twin–chain gel networks (G80, G88, G80SA, G88SA). The functionalization protocol favors the decoration of PVA chains over crosslinking by the sebaceate esters. We found a correlation between the extent of functionalization of P80/88 and the structural or dynamic properties of the obtained twin–chain gels. All the PVA cryogels exhibit a disordered, interconnected sponge-like porosity. In addition, the polymers functionalization produces slightly smaller pores at the microscale, while patterns of dense regions alternated with interconnected porosity are observed in the non-functionalized networks. Finally, the functionalization of PVA increased the capability of the gels to upload organic solvents (e.g. 2-butanone and diethyl carbonate), a relevant improvement to target soil and aged adhesives with different hydrophilicity/hydrophobicity, typically found in restoration interventions on different types works of art, such as paintings, murals, metal, and paper artworks. When gels were applied to remove soil from painting mockups mimicking modern/contemporary painted layers, G80SA showed faster soil removal than G80/88 and G88SA, and a more complete cleaning efficacy after few short applications, likely due to an optimal balance among its porosity, adhesivity and compatibility with hydrophobic substances. Notably, no additional mechanical action was necessary after the removal of the gels. G80SA proved to be the most effective system, performing better than its non-functionalized counterpart, even on rough paints, and water-sensitive surfaces, as demonstrated by the safe and controlled cleaning of a selection of modern/contemporary canvas paintings from Gastone Novelli, Enrico Castellani and Mario Sironi (Peggy Guggenheim Collection, Venice), which exhibited complex and various restoration challenges. Using the new gels allowed safe and, thus, time-effective removal of soil and aged varnish layers that were affecting the artifacts. These enhanced performances improve on the non-decorated PVA/PVA reference and surpass traditional approaches with poorly confined solvents and polymer thickeners, typical benchmarks in the traditional restoration practice, which require

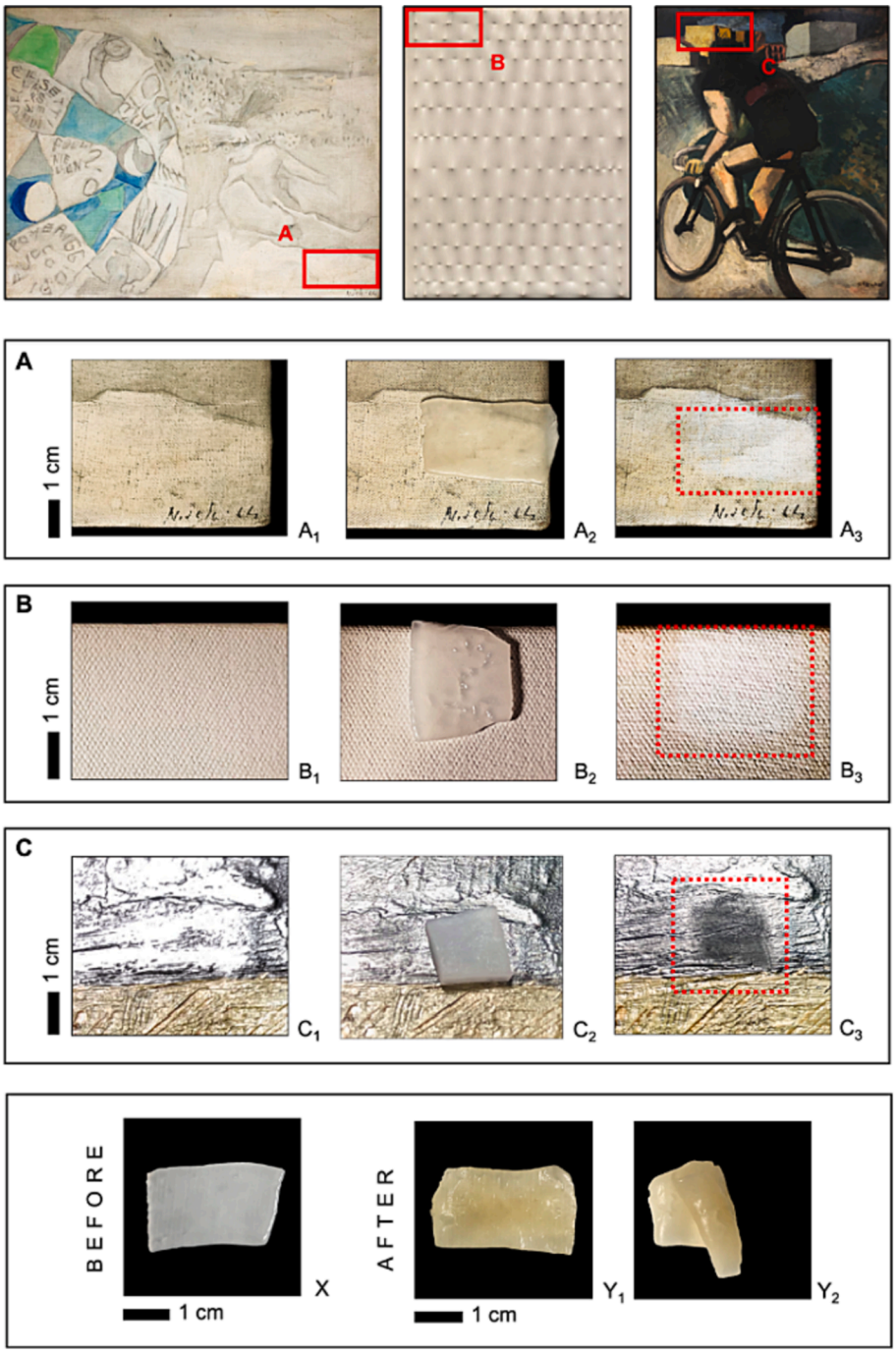

Fig. 8. The three canvas paintings belonging to the Peggy Guggenheim Collection (Venice) cleaned using the G80SA hydrogel. **Top row:** (A) Gastone Novelli "Ha vinto il Bologna" ("The Bologna Team Won the Match", 1964), (B) Enrico Castellani "Superficie Bianca" ("White Surface", 1977) and (C) Mario Sironi "Il ciclista" ("The Cyclist", 1916). **Rows $A_{1\text{-}3}$, $B_{1\text{-}3}$, $C_{1\text{-}3}$:** Details of areas of the paintings before the application of gels ("1"), during the application ("2"), and after gel removal ("3"), showing the removal of soil (A,B) or aged varnish (C) from the painted layers. Images $C_{1\text{-}3}$ were collected under grazing light, where the varnish layer on black color appears as glossy and shining white, to highlight varnish removal and recovery of the original matte color by the gel. **Bottom row:** (X) A G80SA gel before application. ($Y_{1\text{-}2}$) A G80SA after the removal of dirt (1) and aged varnish (2), showing the uptake of dirt/varnish into the gels.

numerous time-consuming cleaning steps to avoid damages to the original painted layers (see Table 4).[8,22].

Overall, functionalization of PVA with sebacic acid proved to be an effective process to formulate a new library of novel twin-chain PVA cryogels with tunable properties and applicative potential in the restoration of artifacts with various surfaces and cleaning issues. In particular, the new gels fill a gap between hydrogels and organogels in art preservation, and candidate as a complementary tool to these systems. In addition, they provide a novel route to introduce bio-derived compounds in PVA cryogels, alternative to the direct replacement of PVA with biopolymers.[30,54] The versatility and feasibility of this functionalization approach will allow applications also in transversal fields to Cultural Heritage conservation, such as biomedicine and tissue engineering, where modulation of polymers and colloidal soft matter with low toxicity and good biocompatibility is a strict requirement.

Table 4
Summary of the advantages of the new PVA TC-decorated gel demonstrated in this contribution, as compared to the main state-of-the-art gels and thickeners used for the cleaning of works of art.

Material	G' [kPa]	Water release [mg cm^{-2}]	Features	Ref.
Agar and Gellan	10–20	33	- High water release - Poor applications on rough surfaces. + Polymeric constituents are bioproduced.	[48,50]
Thickeners (PAA and cellulose ethers)	0.2	Non retentive	- Prone to leave residues that requires invasive cleaning solvents. - High water release	[8,52]
pHEMA / PVP	4–5	15–16	- Low surface adaptivity + Highly controlled water release	[46,50]
PVA / PVP	2	4	- Poor compatibility with organic solvents + Good adaptability to surfaces + Low water release	[46,50,53]
PVA TC	2	21	- Moderate compatibility with organic solvents + Good adaptability to surfaces + Highly effective soil removal	[22]
PVA TC-decorated	0.2	17–23	+ (no major issues detected) + Improved compatibility with solvents ++ Improved adaptivity on surfaces ++ Improved soil removal	This work

CRediT authorship contribution statement

Damiano Bandelli: Conceptualization, Data curation, Formal analysis, Investigation, Methodology, Writing - original draft, Writing - review & editing. **Andrea Casini:** Data curation, Formal analysis, Investigation, Methodology. **Teresa Guaragnone:** Data curation, Formal analysis, Investigation, Methodology. **Michele Baglioni:** Data curation, Formal analysis, Investigation, Methodology, Writing - original draft, Writing - review & editing. **Rosangela Mastrangelo:** Data curation, Formal analysis, Investigation, Methodology, Writing - original draft, Writing - review & editing. **Luciano Pensabene Buemi:** Data curation, Investigation, Methodology. **David Chelazzi:** Conceptualization, Data curation, Formal analysis, Methodology, Writing - original draft, Writing - review & editing. **Piero Baglioni:** Supervision, Conceptualization, Validation, Data curation, Formal analysis, Funding acquisition, Methodology, Project administration, Writing - review & editing.

Declaration of Competing Interest

The authors declare that they have no known competing financial interests or personal relationships that could have appeared to influence the work reported in this paper.

Data availability

Data will be made available on request.

Acknowledgements

Massimo Bricchi (Regional Marketing Manager, Kuraray Europe GmbH) and Kuraray Europe are gratefully aknowledged for providing POVAL™ polymers. This project has received fundings from CSGI (Consorzio per lo Sviluppo dei Sistemi a Grande Interfase, Center for Colloid and Surface Science) and from the European project GREENART (GREen ENdeavor in Art ResToration) under the Horizon Europe Grant Agreement 101060941. Views and opinions expressed are however those of the author(s) only and do not necessarily reflect those of the European Union or the European Research Executive Agency (REA). Neither the European Union nor the granting authority can be held responsible for them.

Appendix A. Supplementary data

Supplementary data to this article can be found online at https://doi.org/10.1016/j.jcis.2023.11.093.

References

[1] M. Baglioni, G. Poggi, D. Chelazzi, P. Baglioni, Advanced Materials in Cultural Heritage Conservation, Molecules 26 (13) (2021) 3967.
[2] A. Walther, Viewpoint: From Responsive to Adaptive and Interactive Materials and Materials Systems: A Roadmap, Adv. Mater. 32 (20) (2020) 1905111.
[3] C. Howell, A. Grinthal, S. Sunny, M. Aizenberg, J. Aizenberg, Designing Liquid-Infused Surfaces for Medical Applications: A Review, Adv. Mater. 30 (50) (2018) 1802724.
[4] A.K. Denisin, B.L. Pruitt, Tuning the Range of Polyacrylamide Gel Stiffness for Mechanobiology Applications, ACS Appl. Mater. Interfaces 8 (34) (2016) 21893–21902.
[5] H. Chen, X. Ren, G. Gao, Skin-Inspired Gels with Toughness, Antifreezing, Conductivity, and Remoldability, ACS Appl. Mater. Interfaces 11 (31) (2019) 28336–28344.
[6] C. Shao, L. Meng, M. Wang, C. Cui, B. Wang, C.-R. Han, F. Xu, J. Yang, Mimicking dynamic adhesiveness and strain-stiffening behavior of biological tissues in tough and self-healable cellulose nanocomposite hydrogels, ACS Appl. Mater. Interfaces 11 (6) (2019) 5885–5895.
[7] L. Baij, J. Hermans, B. Ormsby, P. Noble, P. Iedema, K. Keune, A review of solvent action on oil paint, Herit. Sci. 8 (1) (2020) 43.
[8] A. Casoli, Z. Di Diego, C. Isca, Cleaning painted surfaces: evaluation of leaching phenomenon induced by solvents applied for the removal of gel residues, Environ. Sci. Pollut. Res. 21 (23) (2014) 13252–13263.
[9] A. Casini, D. Chelazzi, P. Baglioni, Advanced methodologies for the cleaning of works of art, Sci. China Technol. Sci. 66 (8) (2023) 2162–2182.
[10] D. Chelazzi, P. Baglioni, From Nanoparticles to Gels: A Breakthrough in Art Conservation Science, Langmuir 39 (31) (2023) 10744–10755.
[11] D. Chelazzi, R. Giorgi, P. Baglioni, Microemulsions, Micelles, and Functional Gels: How Colloids and Soft Matter Preserve Works of Art, Angew. Chem. Int. Ed. 57 (25) (2018) 7296–7303.
[12] P. Baglioni, D. Chelazzi, R. Giorgi, Nanotechnologies in the conservation of cultural heritage: a compendium of materials and techniques, Springer, 2015.
[13] P. Baglioni, D. Berti, M. Bonini, E. Carretti, L. Dei, E. Fratini, R. Giorgi, Micelle, microemulsions, and gels for the conservation of cultural heritage, Adv. Colloid Interface Sci. 205 (2014) 361–371.
[14] C. Mazzuca, G. Poggi, N. Bonelli, L. Micheli, P. Baglioni, A. Palleschi, Innovative chemical gels meet enzymes: A smart combination for cleaning paper artworks, J. Colloid Interface Sci. 502 (2017) 153–164.
[15] C. Mazzuca, L. Micheli, M. Carbone, F. Basoli, E. Cervelli, S. Iannuccelli, S. Sotgiu, A. Palleschi, Gellan hydrogel as a powerful tool in paper cleaning process: A detailed study, J. Colloid Interface Sci. 416 (2014) 205–211.
[16] G. Poggi, H.D. Santan, J. Smets, D. Chelazzi, D. Noferini, M.L. Petruzzellis, L. Pensabene Buemi, E. Fratini, P. Baglioni, Nanostructured bio-based castor oil organogels for the cleaning of artworks, J. Colloid Interface Sci. 638 (2023) 363–374.
[17] A. Zuliani, D. Bandelli, D. Chelazzi, R. Giorgi, P. Baglioni, Environmentally friendly ZnO/Castor oil polyurethane composites for the gas-phase adsorption of acetic acid, J. Colloid Interface Sci. 614 (2022) 451–459.
[18] A. Zuliani, D. Chelazzi, R. Mastrangelo, R. Giorgi, P. Baglioni, Adsorption kinetics of acetic acid into ZnO/castor oil-derived polyurethanes, J. Colloid Interface Sci. 632 (2023) 74–86.
[19] L. Campanella, R. Angeloni, F. Cibin, E. Dell'Aglio, F. Grimaldi, R. Reale, M. Vitali, Capsulated essential oil in gel spheres for the protection of cellulosic cultural heritage, Nat. Prod. Res. 35 (1) (2021) 116–123.
[20] B. Ramírez Barat, E. Cano, P. Letardi, Advances in the design of a gel-cell electrochemical sensor for corrosion measurements on metallic cultural heritage, Sens. Actuators B 261 (2018) 572–580.
[21] L. Pensabene Buemi, M.L. Petruzzellis, D. Chelazzi, M. Baglioni, R. Mastrangelo, R. Giorgi, P. Baglioni, Twin-chain polymer networks loaded with nanostructured

fluids for the selective removal of a non-original varnish from Picasso's "L'Atelier" at the Peggy Guggenheim Collection, Venice, Herit. Sci. 8 (1) (2020) 77.
[22] R. Mastrangelo, D. Chelazzi, G. Poggi, E. Fratini, L. Pensabene Buemi, M. L. Petruzzellis, P. Baglioni, Twin-chain polymer hydrogels based on poly(vinyl alcohol) as new advanced tool for the cleaning of modern and contemporary art, Proc. Natl. Acad. Sci. U.S.A. 117 (13) (2020) 7011–7020.
[23] F. Di Turo, L. Medeghini, How Green Possibilities Can Help in a Future Sustainable Conservation of Cultural Heritage in Europe, Sustainability 13 (7) (2021) 3609.
[24] M. Teodorescu, M. Bercea, S. Morariu, Biomaterials of PVA and PVP in medical and pharmaceutical applications: Perspectives and challenges, Biotechnol. Adv. 37 (1) (2019) 109–131.
[25] M. Aslam, M.A. Kalyar, Z.A. Raza, Polyvinyl alcohol: A review of research status and use of polyvinyl alcohol based nanocomposites, Polym. Eng. Sci. 58 (12) (2018) 2119–2132.
[26] F. Kawai, X. Hu, Biochemistry of microbial polyvinyl alcohol degradation, Appl. Microbiol. Biotechnol. 84 (2) (2009) 227–237.
[27] Y.-N. Chen, L. Peng, T. Liu, Y. Wang, S. Shi, H. Wang, Poly(vinyl alcohol)–Tannic Acid Hydrogels with Excellent Mechanical Properties and Shape Memory Behaviors, ACS Appl. Mater. Interfaces 8 (40) (2016) 27199–27206.
[28] C. Hu, Y. Zhang, X. Wang, L. Xing, L. Shi, R. Ran, Stable, Strain-Sensitive Conductive Hydrogel with Antifreezing Capability, Remoldability, and Reusability, ACS Appl. Mater. Interfaces 10 (50) (2018) 44000–44010.
[29] M.D. Pianorsi, M. Raudino, N. Bonelli, D. Chelazzi, R. Giorgi, E. Fratini, P. Baglioni, Organogels for the cleaning of artifacts, Pure Appl. Chem. 89 (1) (2017) 3–17.
[30] V. Rosciardi, D. Chelazzi, P. Baglioni, "Green" biocomposite Poly (vinyl alcohol)/starch cryogels as new advanced tools for the cleaning of artifacts, J. Colloid Interface Sci. 613 (2022) 697–708.
[31] A.K. Sonker, N. Tiwari, R.K. Nagarale, V. Verma, Synergistic effect of cellulose nanowhiskers reinforcement and dicarboxylic acids crosslinking towards polyvinyl alcohol properties, J. Polym. Sci. A Polym. Chem. 54 (16) (2016) 2515–2525.
[32] T. Kanda, M. Kitawaki, T. Arata, Y. Matsuki, T. Fujiwara, Structural analysis of cross-linked poly(vinyl alcohol) using high-field DNP-NMR, RSC Adv. 10 (14) (2020) 8039–8043.
[33] S. Jian, S. Xiao Ming, Crosslinked PVA-PS thin-film composite membrane for reverse osmosis, Desalination 62 (1987) 395–403.
[34] A. Casini, D. Chelazzi, R. Giorgi, Jin Shofu Starch Nanoparticles for the Consolidation of Modern Paintings, ACS Appl. Mater. Interfaces 13 (31) (2021) 37924–37936.
[35] R.K. Tubbs, Sequence distribution of partially hydrolyzed poly(vinyl acetate), J. Polym. Sci. A Polym. Chem. 4 (3) (1966) 623–629.
[36] G. Van der Velden, J. Beulen, 300-MHz Proton NMR and 25-MHz carbon-13 NMR investigations of sequence distributions in vinyl alcohol-vinyl acetate copolymers, Macromolecules 15 (4) (1982) 1071–1075.
[37] B.D. Coleman, T.G. Fox, General theory of stationary random sequences with applications to the tacticity of polymers, J. Polym. Sci. A Polym. Chem. 1 (10) (1963) 3183–3197.
[38] A. Lederer, J. Brandt, Chapter 2 - Multidetector size exclusion chromatography of polymers, in: M.I. Malik, J. Mays, M.R. Shah (Eds.), Molecular Characterization of Polymers, Elsevier, 2021, pp. 61–96.
[39] J.E. Puskas, W. Burchard, A.J. Heidenreich, L.D. Santos, Analysis of branched polymers by high resolution multidetector size exclusion chromatography: Separation of the effects of branching and molecular weight distribution, J. Polym. Sci. A Polym. Chem. 50 (1) (2012) 70–79.
[40] A. Monaco, B. Drain, C.R. Becer, Detailed GPC analysis of poly(N-isopropylacrylamide) with core cross-linked star architecture, Polym. Chem. 12 (36) (2021) 5229–5238.
[41] D.M. Meunier, J.W. Lyons, J.J. Kiefer, Q.J. Niu, L.M. DeLong, Y. Li, P.S. Russo, R. Cueto, N.J. Edwin, K.J. Bouck, H.C. Silvis, C.J. Tucker, T.H. Kalantar, Determination of Particle Size Distributions, Molecular Weight Distributions, Swelling, Conformation, and Morphology of Dilute Suspensions of Cross-Linked Polymeric Nanoparticles via Size-Exclusion Chromatography/Differential Viscometry, Macromolecules 47 (19) (2014) 6715–6729.
[42] B.M. Tande, N.J. Wagner, M.E. Mackay, C.J. Hawker, M. Jeong, Viscosimetric, Hydrodynamic, and Conformational Properties of Dendrimers and Dendrons, Macromolecules 34 (24) (2001) 8580–8585.
[43] P. Levitz, Toolbox for 3D imaging and modeling of porous media: Relationship with transport properties, Cem. Concr. Res. 37 (3) (2007) 351–359.
[44] P. Levitz, D. Tchoubar, Disordered porous solids : from chord distributions to small angle scattering, J. Phys. I 2 (6) (1992) 771–790.
[45] S.D. Hudson, J.L. Hutter, M.-P. Nieh, J. Pencer, L.E. Millon, W. Wan, Characterization of anisotropic poly(vinyl alcohol) hydrogel by small- and ultra-small-angle neutron scattering, J. Chem. Phys. 130 (3) (2009), 034903.
[46] M. Baglioni, J.A.L. Domingues, E. Carretti, E. Fratini, D. Chelazzi, R. Giorgi, P. Baglioni, Complex Fluids Confined into Semi-interpenetrated Chemical Hydrogels for the Cleaning of Classic Art: A Rheological and SAXS Study, ACS Appl. Mater. Interfaces 10 (22) (2018) 19162–19172.
[47] J.A.L. Domingues, N. Bonelli, R. Giorgi, E. Fratini, F. Gorel, P. Baglioni, Innovative Hydrogels Based on Semi-Interpenetrating p(HEMA)/PVP Networks for the Cleaning of Water-Sensitive Cultural Heritage Artifacts, Langmuir 29 (8) (2013) 2746–2755.
[48] C. Mazzuca, L. Micheli, E. Cervelli, F. Basoli, C. Cencetti, T. Coviello, S. Iannuccelli, S. Sotgiu, A. Palleschi, Cleaning of Paper Artworks: Development of an Efficient Gel-Based Material Able to Remove Starch Paste, ACS Appl. Mater. Interfaces 6 (19) (2014) 16519–16528.
[49] N. Bonelli, C. Montis, A. Mirabile, D. Berti, P. Baglioni, Restoration of paper artworks with microemulsions confined in hydrogels for safe and efficient removal of adhesive tapes, Proc. Natl. Acad. Sci. U.S.A. 115 (23) (2018) 5932–5937.
[50] J. Domingues, N. Bonelli, R. Giorgi, P. Baglioni, Chemical semi-IPN hydrogels for the removal of adhesives from canvas paintings, Appl. Phys. A 114 (3) (2014) 705–710.
[51] C.E. Dillon, A.F. Lagalante, R.C. Wolbers, Acrylic emulsion paint films: The effect of solution pH, conductivity, and ionic strength on film swelling and surfactant removal, Stud. Conserv. 59 (1) (2014) 52–62.
[52] E. Fratini, E. Carretti, Cleaning IV: Gels and Polymeric Dispersions, in: P. Baglioni, D. Chelazzi (Eds.), Nanoscience for the Conservation of Works of Art, The Royal Society of Chemistry, 2013.
[53] N. Bonelli, G. Poggi, D. Chelazzi, R. Giorgi, P. Baglioni, Poly(vinyl alcohol)/poly (vinyl pyrrolidone) hydrogels for the cleaning of art, J. Colloid Interface Sci. 536 (2019) 339–348.
[54] V. Rosciardi, P. Baglioni, Role of amylose and amylopectin in PVA-starch hybrid cryo-gels networks formation from liquid-liquid phase separation, J. Colloid Interface Sci. 630 (2023) 415–425.